The Incomplete Transformation Phenomenon in Steel

H.I. AARONSON, W.T. REYNOLDS, Jr., and G.R. PURDY

The incomplete transformation (ICT) phenomenon is defined as the temporary cessation of ferrite formation (in the absence of carbide precipitation at α:γ boundaries) before the fraction of austenite transformed to ferrite predicted by the Lever rule is attained. The ICT phenomenon is central to the ''overall reaction kinetics'' definition of bainite but plays lesser roles in the quite different groups of phenomena comprising the ''surface relief'' and ''generalized microstructural'' definitions. Experimental generalizations that can be made about the ICT are briefly noted. Effects of alloying elements, X, upon various aspects of the nucleation and growth of ferrite are listed in order of apparently increasing strength. The ICT is seen to be one of the stronger effects in the latter spectrum. Theories of the ICT are then critically examined. The currently most promising theories involve (1) the cessation of growth induced by the coupled-solute drag effect (C-SDE), accentuated by the overlap of the carbon diffusion fields associated with adjacent ferrite crystals; and (2) the concepts of item (1) plus local alloying element partition between ferrite and austenite (LE-NP), thereby making any further ferrite growth require volume diffusion of X in austenite and thus to take place exceedingly slowly. Distinguishing between these theories will require use of an Fe-C-X system in which the temperature-carbon concentration paths of the paraequilibrium (PE) Ae_3 and of the ''no partition'' boundary are well separated. Although the Fe-C-Mo system has proved convenient for studying many aspects of the ICT phenomenon, it does not fulfill this specification. Fe-C-Mn alloys do so and should be particularly useful subjects for future investigations of the ICT phenomenon.

I. INTRODUCTION

THE incomplete transformation phenomenon, discovered by Wever and Lange[1] in 1932, has been described as the formation of significantly less than the Lever rule proportion of ferrite in the absence of carbide precipitation.[2] The overall reaction kinetics definition of bainite[3,4] ascribes to this transformation product its own C-shaped time-temperature-transformation (TTT) curve for the initiation of transformation, with the transformation to ferrite becoming increasingly incomplete as the upper temperature limit of this curve is approached[3] (Figures 1(a) and (b)). Zener[5] has proposed that this limit is the T_o temperature. Figure 2 shows decisively that this is not so, at least in the Fe-C-Mo system.[6]

Inasmuch as international agreement on the definition of bainite has yet to be reached despite approximately 75 years of research, the other two principal definitions currently in use should be noted. One is the surface relief definition, wherein any plate-shaped (or lath-shaped) transformation product, formed above the martensite temperature range, that exhibits an invariant plane strain surface relief effect may be described as bainite. (On this view, distinguishing between martensite and bainite can thus be problematic, particularly below the M_d temperature, the highest temperature at which martensite can form in deformed austenite.)

The original microstructural definition of bainite[7,8] is Widmanstätten ferrite plates or laths with carbide precipitation at the austenite:ferrite boundaries. This definition has been subsequently generalized as a nonlamellar, competitive eutectoid reaction in which the eutectoid phases can have any morphology other than the alternating plates characteristic of pearlite.[4,9]

Although claims to the contrary have been made,[10] and refuted,[11,12] these three definitions are often in conflict. A microstructure that is bainite on one definition may thus not be bainite on either or both of the other two definitions.[11,12]

In this article, we will first summarize the experimental generalizations that have been made about the incomplete transformation (ICT) phenomenon. An attempt will then be made to situate ICT within the spectrum of effects of alloying elements upon ferrite formation. Both of these sections have been condensed from a recent lengthy overview of these phenomena.[13] The remainder of the article will be focused upon critically reviewing the various theories that have been proposed for the ICT.

II. EXPERIMENTAL GENERALIZATIONS ON ICT PHENOMENA

The following are key generalizations that have been made in a detailed overview of the overall reaction kinetics definition of bainite.[13] Experimental evidence or theory of special importance is briefly noted.

(A) ICT is not a generally occurring phenomenon in Fe-C-X alloys.[14] Figure 3 shows that the ICT occurs in Fe-C-Mo alloys only when the proportions of Mo and C exceed critical proportions.[14] ICT is found in C-rich and X-rich alloys when X = Ni[18] and Mn[19] but is apparently absent when X = Co and Cu.[19]

H.I. AARONSON, formerly R.F. Mehl University Professor Emeritus, Department of Materials Science and Engineering, Carnegie Mellon University, Pittsburgh, PA, 15213-3890, and Visiting Professor, School of Physics and Materials Engineering, Monash University, Victoria 3800, Australia, is deceased. W.T. REYNOLDS, Jr., Professor, is with the Department of Materials Science and Engineering, Virginia Tech, Blacksburg, VA, 24061-0237. Contact e-mail: reynolds@vt.edu G.R. PURDY, University Professor Emeritus, is with the Department of Materials Science and Engineering, McMaster University, Hamilton, ON, Canada L8S 4L7.

This article is based on a presentation made in the ''Hillert Symposium on Thermodynamics & Kinetics of Migrating Interfaces in Steels and Other Complex Alloys,'' December 2–3, 2004, organized by The Royal Institute of Technology in Stockholm, Sweden.

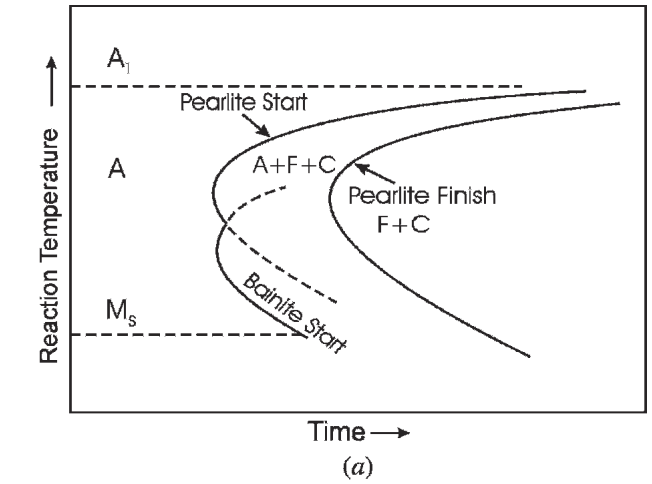

(*a*)

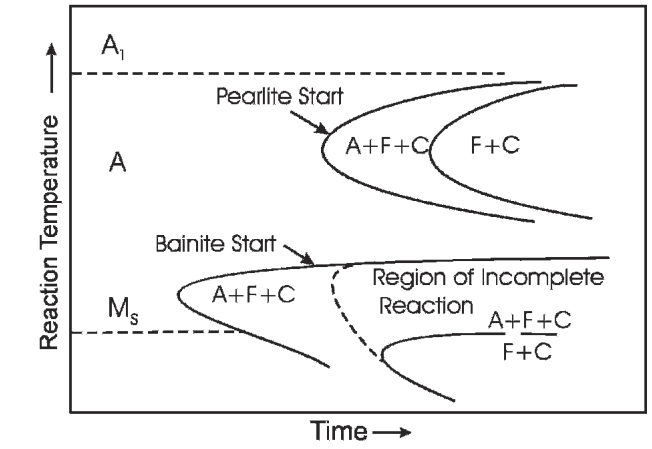

(*b*)

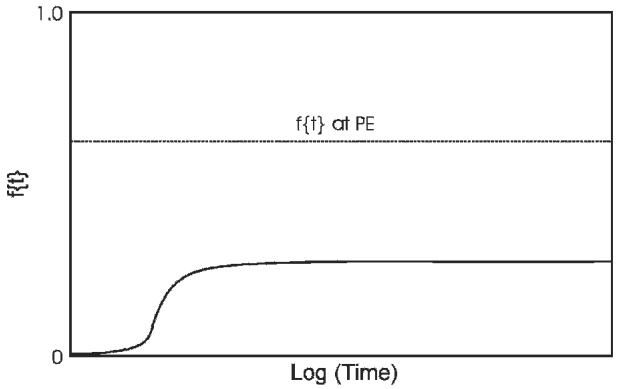

(*c*)

Fig. 1—(*a*) TTT diagram for a plain carbon steel in which the pearlite region heavily overlaps that of overall-reaction-kinetics bainite.[3] (*b*) TTT diagram for high alloy steel in which the pearlite and overall-reaction-kinetics bainite regions are widely separated. (*c*) Schematic plot of fraction of bainite transformed to overall-reaction-kinetics bainite, illustrating the presence of a stasis region wherein transformation has halted.

(B) A bay in the TTT curve for the beginning of transformation in a given Fe-C-X alloy does not necessarily mean that ICT occurs in this alloy.[14]

(C) In Fe-C-X systems wherein ICT has been observed, this phenomenon occurs over a wider temperature range at a given pct X with increasing pct C[14] and at a given pct C with increasing pct X.[14,15]

(D) At a given pct C, ICT appears to occur over a wider temperature range as the Wagner interaction parameter, $\varepsilon_{12}^{\gamma}$,* becomes increasingly negative, and also, but much more slowly, when $\varepsilon_{12}^{\gamma}$ is increasingly positive.[13]

When $\varepsilon_{12}^{\gamma}$ is similar for two X's, the one having a larger size difference with respect to Fe will have the

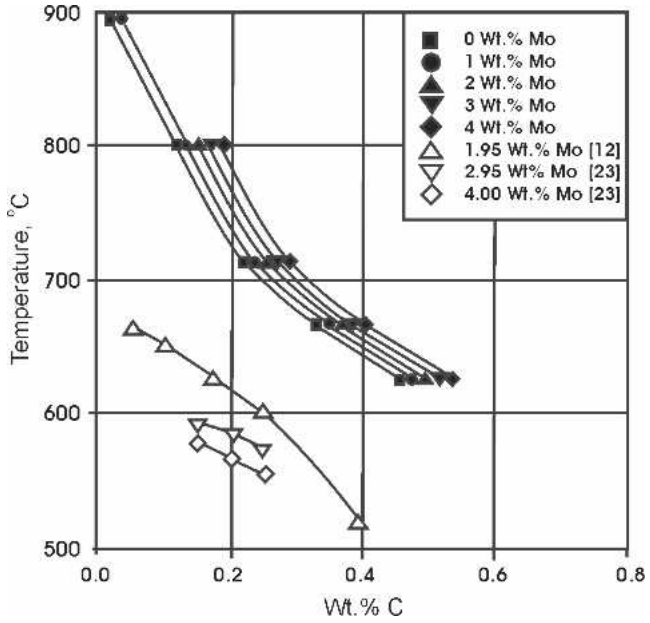

Fig. 2—Calculated plots of T_o *vs* pct C at different wt pct Mo, compared with experimental data on the k-B_s (kinetic bainite-start) temperature for three Fe-C-Mo alloys.[6]

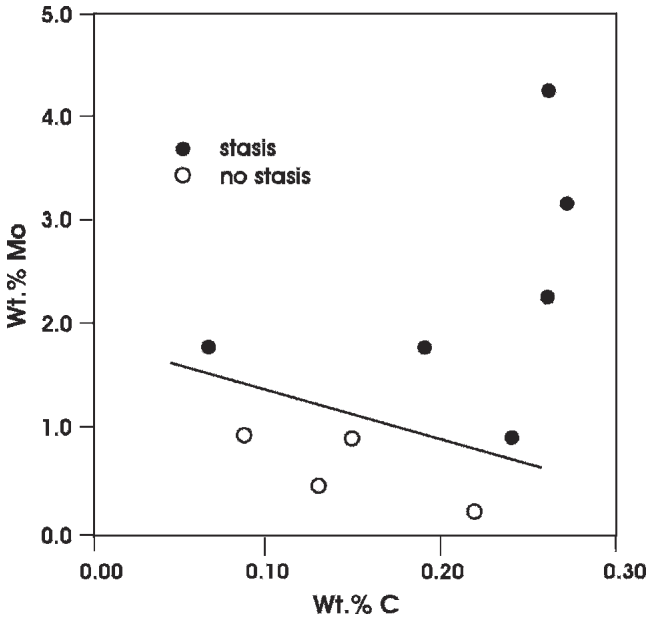

Fig. 3—Wt pct Mo *vs* wt pct C region within which incomplete transformation has been found at any reaction temperature.[14]

*$\varepsilon_{12}^{\gamma}$ is the Wagner interaction parameter, 1 represents C and 2 denotes X.

stronger manifestations of the ICT.[13] These effects can be explained as a coupled solute drag effect (C-SDE).[12,14,20,22–24]

(E) Carbide precipitation at austenite:ferrite boundaries is absent until after transformation has resumed at the end of the interval of incomplete transformation (*i.e.*, stasis).[14,20,66–68]

III. INFLUENCE OF X UPON FERRITE FORMATION IN FE-C-X ALLOYS[13]

Except for the first effect, these effects are listed in order of increasing influence of X that cannot be ascribed to shifting of the paraequilibrium (PE) Ae_3. Estimation of the relative strength of the various effects is based upon the considerations of (D) in Section II and of the concentrations of C and X needed to produce a detectable amount of each effect.

A. *Effect of X upon the Widmanstätten Start Temperature[21]*

As long as the Widmanstätten start temperature (W_s) is fairly high, this effect appears due only to X shifting the PE Ae_3 curve upward and sideways or downward and sideways.[21]

B. *Influence of X upon the Aspect Ratio of Grain Boundary Allotriomorphs[25,26]*

When X = Al, Mn, Si, Cu, Co, or Ni, this ratio is about 1/3, independent of the X concentration, reaction temperature, and reaction time (prior to extensive overlap of carbon diffusion fields associated with adjacent ferrite crystals).[25] However, when X = V, this ratio is often very small.[26] These observations are not yet understood.

C. *Influence of X upon the Growth Kinetics of Grain Boundary Allotriomorphs[25–28]*

Although shifting of the PE Ae_3 can explain some of the alloying element effects upon the parabolic rate constant for allotriomorph thickening, reductions of this constant to values smaller than predicted for PE are well documented and are primarily associated with the Wagner interaction parameter, $\varepsilon_{12}^{\gamma}$, and the C-SDE, as emphasized in (D) in Section II.

D. *Influence of X upon the Nucleation Rate of Grain Boundary Allotriomorphs[29]*

When X = Co, Si, and Mo (at temperatures above the ''nose'' in the TTT diagram), the effect of X upon the nucleation rate at a given driving force can be explained in terms of PE Ae_3 shifting. Only when X = Ni and Mn are significant effects exerted by other factors. These are deduced to be decreasing the volume free energy change driving nucleation, and, at least in the case of Mn, also decreasing the grain boundary energy more than the austenite:ferrite boundary energies.

E. *Formation of a Bay in the TTT Curve for the Beginning of Transformation*

Whereas the ORK definition of bainite requires that a bay be present in the TTT curve for initiation of ferrite formation in Fe-C and in all hypoeutectoid Fe-C-X alloys, this generalization has not been borne out experimentally at all bulk C and X concentrations studied in either an Fe-0.80 pct C-0.77 pct Mn alloy[30] or in Fe-C-X alloys in the temperature range where bulk partition of X between austenite and ferrite is absent and X = Si,[19,31,32] Al,[31,32] Co,[19,31,32] Cu,[19,28,31] Mn,[19,31] Ni,[19,31] and Pt.[31]

F. *Degenerate Ferrite Formation at Temperatures below the Bay*

These irregularly shaped ferrite crystals have been found in Fe-C-Cr[15,20] and more pronouncedly in Fe-C-Mo alloys.[12,14,33] The transmission electron microscopy (TEM) observations[14] and recent three-dimensional reconstructions from multiple sectioning[34,35] have shown that such structures actually consist of packets of sympathetically nucleated needles/laths, usually nucleated side-by-side, but less frequently edge-to-side, *i.e.,* a new packet is formed at an angle with respect to one already present.

G. *Incomplete Transformation*

The isothermal transformation temperature and time region during which both nucleation and growth cease prior to the formation of the PE proportion of ferrite is known as ''stasis'' (Figure 1(c) and all items in Section II).

H. *Formation of Twin Boundary Allotriomorphs**

These have so far been found only when X = Cr,[15] Mo,[12,14] and W.[34]

I. *Wrinkled Ferrite**

*A judgment of the relative strength of these effects with respect to that of Section III–G (ICT) cannot be made on the basis of the information available.

Originally observed by Hultgren as dark-etching ferrite allotriomorphs that have a wrinkled appearance,[36] Brown *et al.*[37] have used TEM to show that in an Fe-C-Mo alloy, allotriomorph interfaces that are irrationally oriented with respect to their parent austenite grain give rise to a high density of dislocations within the allotriomorphs upon which Mo_2C carbides have precipitated. A connection between the dislocations within ferrite and the interphase boundary structure should be sought.

In summary, the incomplete transformation phenomenon appears to be one of the strongest manifestations of an alloying element effect upon ferrite formation in Fe-C-X alloys. This effect must be powerful enough to halt nucleation and growth in the presence of an appreciable fraction of the driving force for these processes. In Section IV, various explanations that have been offered for this restraining force will be considered.

IV. EXPLANATIONS FOR THE INCOMPLETE TRANSFORMATION PHENOMENON

A. *Incomplete Transformation Is Absent Because the Pearlite Reaction Replaces That of Bainite in the ICT Range*

This explanation has long been widely accepted.[3] However, this explanation has been successfully disproved in

some Fe-C-Mn, Fe-C-Si, Fe-C-Ni, and Fe-C-Cu alloys[19] by the use of coarse austenite grain sizes and careful observation of microstructures developed at early stages of transformation.

B. *Shear Theories*

1. *High-velocity shear theories*

a. *Early views*

One of the earliest workers in this field, Robertson,[7] noting that the etched optical microstructure of what would later be termed ''bainite'' becomes darker and more acicular the lower the isothermal reaction temperature, proposed a close connection between the mechanisms of the bainite and martensite reactions. Davenport and Bain[8] viewed bainite plates as formed during a single high-velocity shear. Hillert[34,35,36] has shown, however, that the lengthening kinetics of bainite plates are essentially those allowed by carbon diffusion in austenite, thereby (supposedly) eliminating this concept, though it continues to appear even in exacting current research.[41]

b. *Oblak–Hehemann theory*[42]

Oblak and Hehemann[42] studied the optical and the TEM microstructures of ferrite formed above and below the bay in the TTT curve for the initiation of transformation in complexly alloyed hypoeutectoid steels. Those formed above the bay contained no systematic arrays of dislocations or other substructures. Structures formed below the bay, however, consisted of elongated platelets or ''subunits,'' earlier identified as having been formed by sympathetic nucleation.[43] The subunits were considered to form by high-velocity shear (Figure 4). Accumulated transformation strain energy was taken as responsible for halting the growth of individual subunits. Following a delay time for annealing out of the dislocations thus formed, another ''burst'' of high velocity shear can then occur. Limited thermionic electron emission microscopy evidence, recorded with *in-situ* motion pictures, has shown that neither the lengthening nor the thickening kinetics of individual subunits proceeds significantly more rapidly than allowed by carbon diffusion in austenite.[2] Hot-stage TEM also showed the absence of high-velocity growth. Hillert[40] has remarked that ''. . .it would seem as a very strange coincidence if the rate of nucleation of new steps and their length should give an overall velocity close to what has been calculated from diffusion-control.''

c. *Bhadeshia and Edmonds theory*[*44]

*Although not acknowledged by the authors, this theory is actually that of Zener.[5]

These authors have proposed that bainite grows at such high velocities that the bainite plates remain substantially supersaturated with respect to carbon. ''The bulk of the partitioning of carbon into the residual austenite must occur after the initial formation event. If this represents the true nature of events, the bainite reaction can be expected to cease as soon as the austenite carbon content reaches a critical value, the magnitude of which would be near the T_o curve, depending upon the exact degree of partitioning occurring simultaneously with transformation. Such an interpretation would also explain the incomplete transformation phenomenon since, with decreasing temperature,

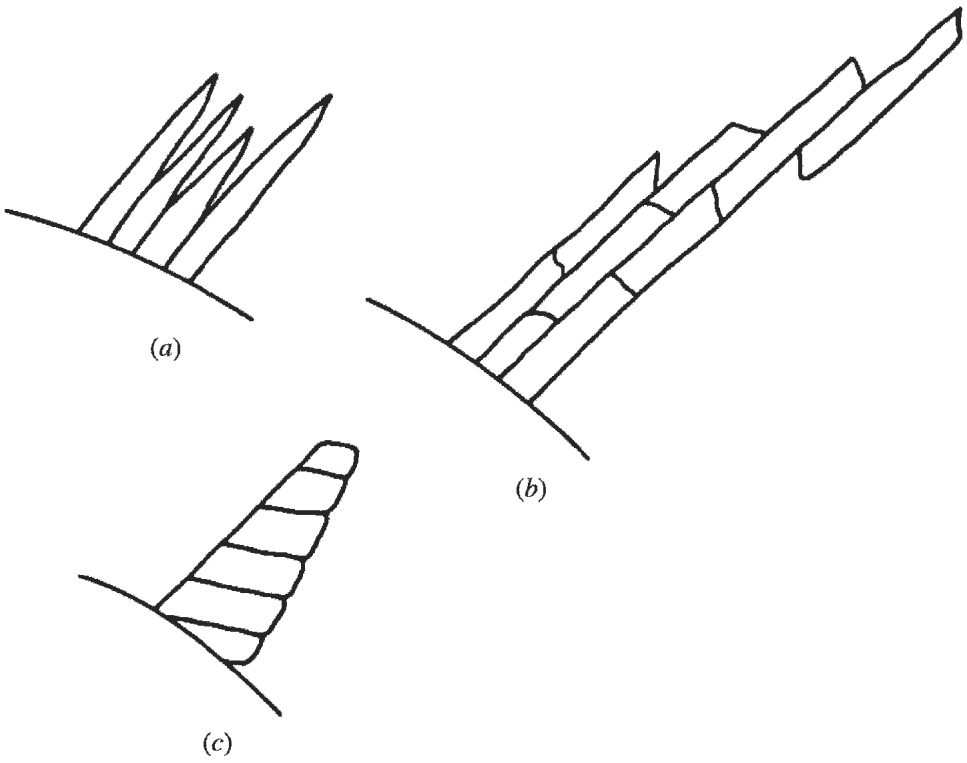

Fig. 4—Versions of the Oblak–Hehemann[42] mechanism for plate formation by repeated nucleation and lateral growth *via* high-velocity shear.

the austenite can tolerate successively greater amounts of carbon before the formation of supersaturated ferrite becomes thermodynamically impossible.''

This theory has been criticized in detail by Aaronson *et al*.[45] Figure 5(a)[45] shows the carbon concentration profiles normal to austenite:ferrite boundaries expected from the Bhadeshia–Edmonds mechanism at successively increasing isothermal reaction times. These profiles fail to recognize that at mobile areas of austenite:ferrite boundaries the chemical potentials of carbon in both phases must be the same. They are similarly inconsistent with the carbon concentration profiles in austenite that must develop as carbon flows away from initially fully supersaturated ferrite in accord with this generalization, as illustrated in Figure 5(b). The concentration profiles associated with diffusion-controlled growth at all stages of the transformation are sketched in Figure 5(c).

Bhadeshia and Edmonds[46] have studied incomplete transformation in an Fe-0.43 pct C-3.00 pct Mn-2.12 pct Si alloy. At 363 °C, quantitative metallography was used to determine that incomplete transformation occurred when the proportion of ferrite reached 52 pct.[44] Assuming that all carbon is transferred to the austenite phase, the average carbon concentration in the austenite follows directly from the pct austenite remaining untransformed during stasis and the bulk carbon concentration in the alloy. Dilatometric data obtained at other reaction temperatures in this alloy[46] permitted calibration of the pct carbon in the untransformed austenite at each temperature. At temperatures greater than or equal to approximately 363 °C, these data points were in good agreement with the T_o *vs* pct C curve (Figure 6). At lower temperatures, the back-calculated carbon concentrations in the untransformed austenite were sometimes appreciably above the T_o *vs* pct C curve, but were always well below the extrapolated PE Ae_3 boundary that would be anticipated in the absence of a C-SDE. Figure 6 shows that when the T_o curve is recalculated with Thermo-Calc, it lies at much higher temperatures and largely destroys the agreement reported by Bhadeshia and Edmonds.[44]

Results similar to those of Bhadeshia and Edmonds were reported on pools of retained austenite after ''austenitizing'' within the $\alpha + \gamma$ region and then isothermal reacting at diverse lower temperatures in Fe-0.11 pct C-1.53 pct Mn-1.50 pct Si,[44] Fe-0.29 pct C-1.40 pct Mn-1.50 pct Si,[5] and Fe-0.16 pct C-1.30 pct Mn-0.38 pct Si[45] alloys when the T_o *vs* pct C curves were obtained from Thermo-Calc. However, in a ductile cast iron containing 3.2 pct C, 2.4 pct Si, 0.21 pct Mn, 0.59 pct Ni, 0.62 pct Cu, and 0.13 pct Mo,[46] the carbon concentration in blocky retained austenite regions corresponded to the T_o curve, whereas those in the thin films of austenite within sheaves correspond to the PE Ae_3 curve.

In order to test this theory on ternary alloys in which the progress of transformation was traced by means of quantitative metallography (point counting), two Fe-C-Mo alloys, Fe-0.24 pct C-0.93 pct Mo and Fe-0.064 pct C-1.80 pct Mo,

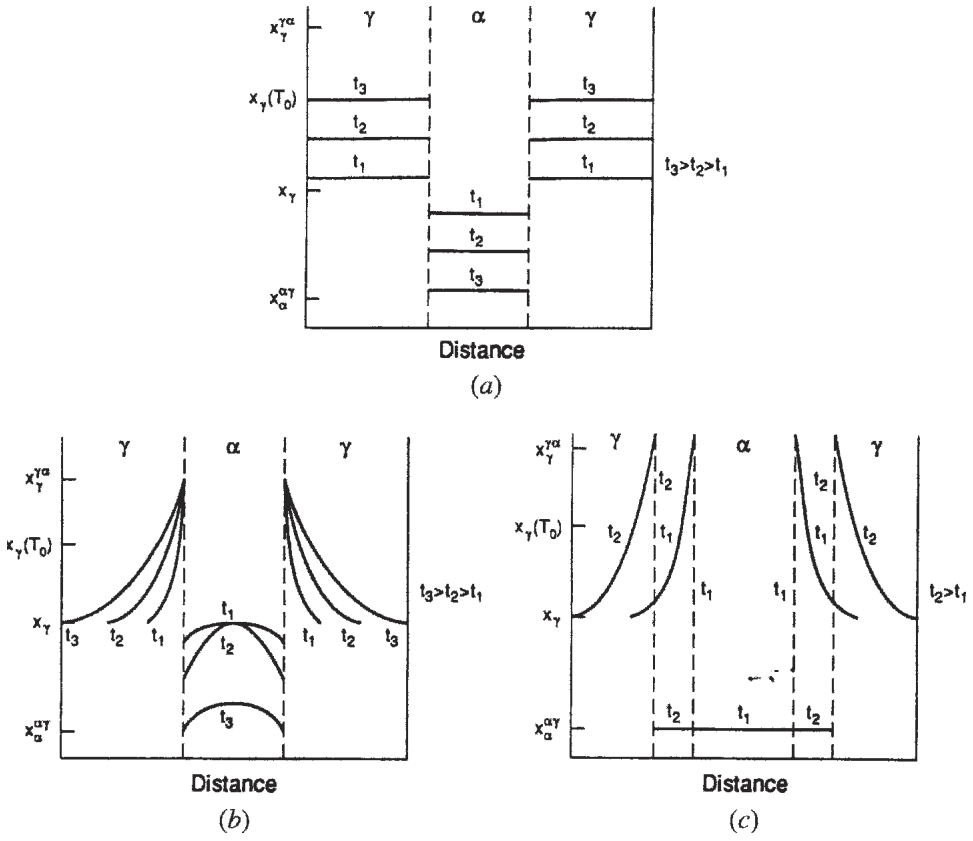

Fig. 5—Concentration-penetration (C-P) curves through a ferrite plate and the adjacent austenite associated with the Bhadeshia–Edmonds[44] mechanism of plate formation by shear. (*a*) C-P curves derived from the Bhadeshia–Edmonds mechanism. (*b*) C-P curves for the Bhadeshia–Edmonds mechanism when equality of chemical potentials at α:γ boundaries is taken into account. (*c*) C-P curves for diffusional growth of ferrite plates.[4]

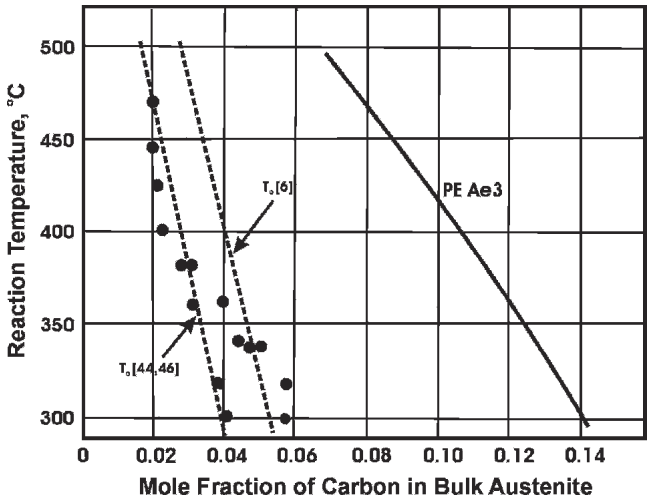

Fig. 6—Comparison of Bhadeshia–Edmonds[42,44] growth mechanism prediction of the carbon concentration in untransformed austenite at stasis with the T_o curve originally reported and that determined during the present investigation.

were selected from the nine studied by Reynolds *et al.*,[14] in which the stasis plateau was particularly pronounced (Figure 7). The data points in Figures 8 and 9 show the carbon concentrations in untransformed austenite (martensite after quenching to room temperature) during the stasis regime at the reaction temperatures studied in these two alloys, using a plotting scale similar to that employed by Bhadeshia and Edmonds. Figures 10 and 11 provide plots of these data on a finer scale. While the T_o *vs* pct C and the back-calculated pct C in austenite curves in Figure 10 are approximately parallel, the experimental data points lie from 0.10 to 0.15 pct C below the calculated curve in this 0.24 pct C alloy. In Figure 11, the two curves have quite different shapes, and differences in the two curves range from 0.25 to 0.37 pct C in the 0.064 pct C alloy. In addition, the difference between T_o and the kinetic bainite start temperature in these two alloys—a measure of the deviation between theory and experiment—is highly sensitive to the carbon concentration in the untransformed austenite (Figures 12 and 13). These absences of agreement are to be expected from the difference between the assumed high-velocity growth kinetics of ferrite plates and those experimentally observed.[38,39,40]

2. *Diffusion-controlled shear theories*

In the 1952 observation by Ko and Cottrell,[50] hot-stage optical microscopy showed that a martensite-like surface relief effect is associated with bainite formed at a low reaction temperature. This work also demonstrated that bainite grows slowly rather than at the high velocities expected of martensite formed in steel. In a subsequent article, Ko[51] showed that proeutectoid ferrite plates produce a similar surface relief effect, whereas grain boundary allotriomorphs yield only surface rumpling. These plates were thus deduced to grow by shear taking place slowly at rates controlled by carbon diffusion in austenite.[50,51] Demonstration with *in-situ* thermionic electron emission microscopy that ferrite plate thickening takes place by the ledge mechanism—as shown by plateaus in plots of half-thickness *vs* isothermal

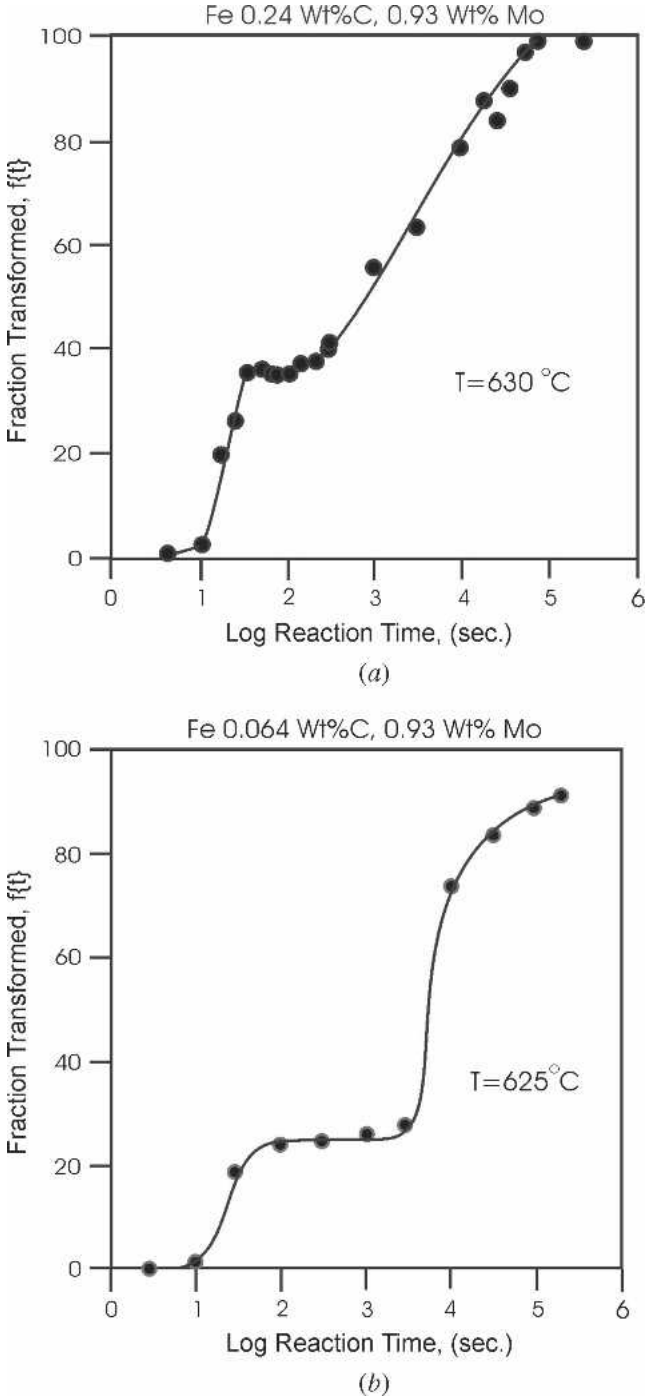

Fig. 7—Isothermal transformation curves exhibiting stasis in two Fe-C-Mo alloys.[14]

reaction time—indicates that the terraces connecting growth ledges are immobile.[49] The TEM has shown that the broad faces of ferrite plates have a sessile structure consisting of structural disconnections (ledges) and misfit dislocations in edge or in mixed orientation.[50,15,52] Recently, some ferrite plate/lath broad faces were found to have a quite different structure, consisting of two sets of screw dislocations[56] whose configuration is the same as that found by Sandvik and Wayman[57] on the broad faces of martensite laths in an Fe-Ni-Mn alloy. However, hot-stage optical microscopy

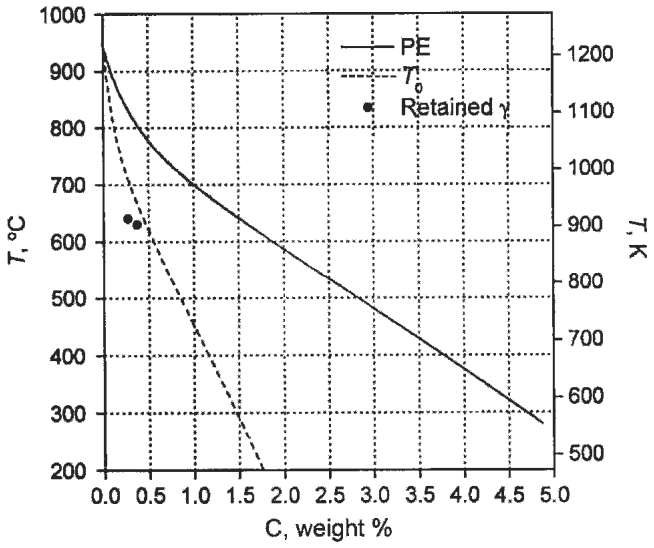

Fig. 8—Comparison of pct C in untransformed austenite at stasis with the T_o curve for an Fe-0.24 wt pct 0.93 wt pct Mo alloy,[14] using a condensed scale.

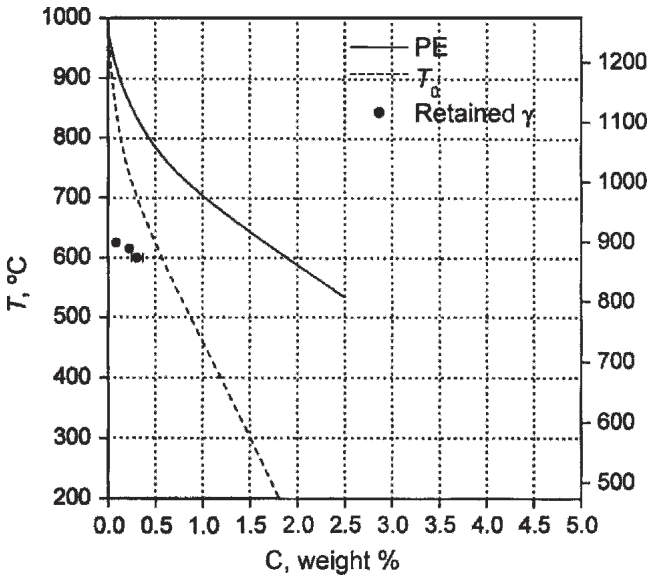

Fig. 9—Same as Figure 8 for Fe-0.064 wt pct C-1.80 wt pct Mo.[14]

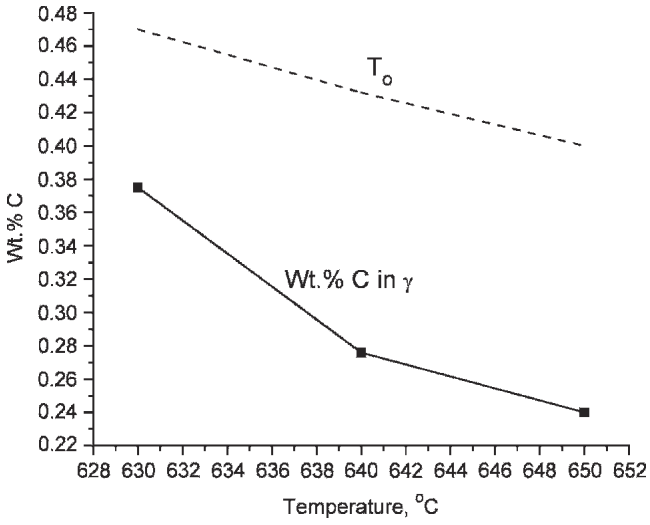

Fig. 10—Back-calculated pct C in untransformed austenite at stasis in Fe-0.24 wt pct C-0.93 wt pct Mo, using an enlarged scale.

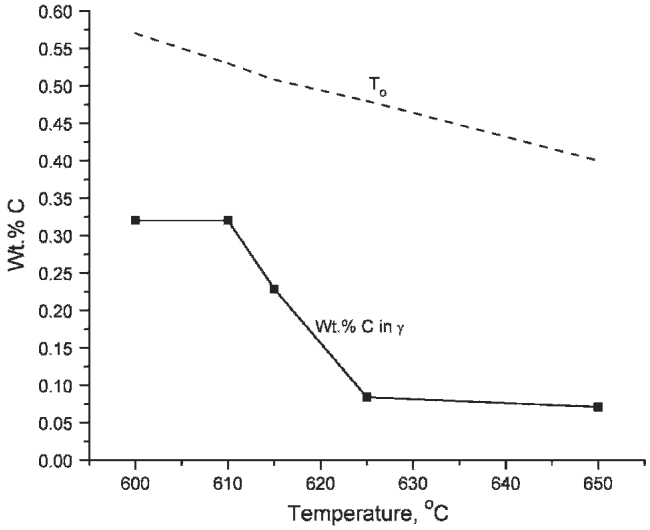

Fig. 11—Back-calculated pct C in untransformed austenite at stasis in Fe-0.064 wt pct C-1.80 wt pct Mo, using an enlarged scale.

measurements on the lengthening kinetics of ferrite/bainite plates conducted over wide temperature ranges in Fe-C alloys provide no evidence for growth faster than carbon diffusion control would allow.[58] Inasmuch as thickening of these plates occurs more than an order of magnitude less rapidly than lengthening (as judged by the aspect ratio of these plates), a strong barrier to growth must exist at the two sets of screw interfaces. This outcome is not consistent with a diffusion-controlled shear mechanism.

C. *Transformation Strain Energy–Induced Incomplete Transformation*

Bouaziz *et al.*[59] have demonstrated that the shape change accompanying bainite formation is accompanied by plastic deformation. On this basis, Quidort *et al.*[60] have proposed that the plastic resistance of the austenite is responsible for incomplete transformation. However, formation of ferrite and bainite plates/laths is often accompanied by a tent-shaped surface relief[52,61–64] rather than the invariant plane strain relief associated with martensite. Tent-shaped reliefs do not produce any deflection of scratches or of interference fringes on opposite sides of a ferrite plate.[63] Hence, there is no shear strain energy associated with such reliefs. As Eshelby[65] has pointed out, the strain energy accompanying martensite plate formation produced by the volume change is much less than that derived from the shape strain. Similar ratios are expected to prevail during the formation of ferrite laths and plates.

Although the stasis times associated with the two Fe-C-Mo alloys discussed in Section IV–B–1–c are relatively short, Hehemann and Troiano[3] have found that stasis times

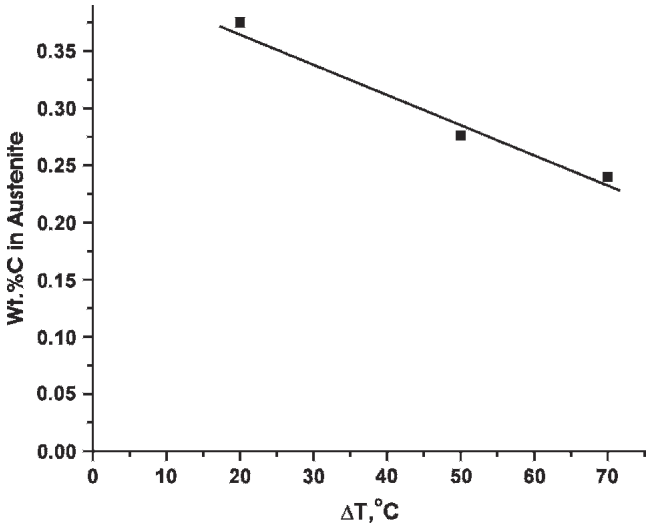

Fig. 12—Difference, ΔT, between T_o and the k-B_s at experimentally based values of pct C in untransformed austenite at stasis in Fe-0.24 wt pct C-0.93 wt pct Mo.

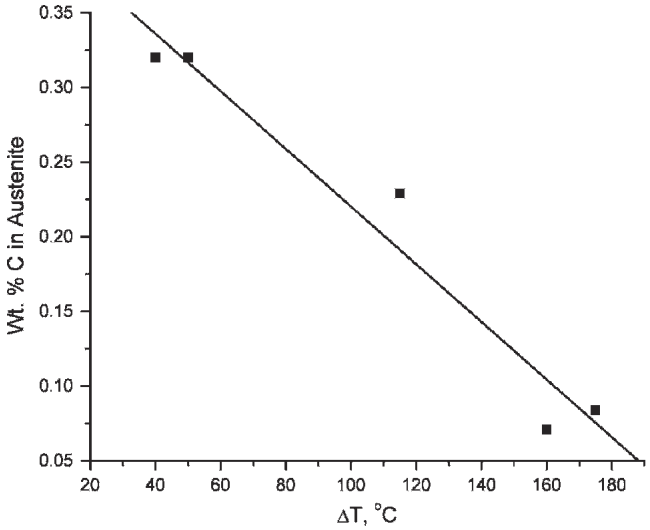

Fig. 13—Difference, ΔT, between T_o and the k-B_s at experimentally based values of pct C in untransformed austenite at stasis in Fe-0.064 pct C-1.80 pct Mo.

can extend for many hours or even days in suitably alloyed steels. Hence, extensive recovery of the deformed austenite matrix is to be expected. This is inconsistent with the maintenance of stasis for times of the order of a day.[3]

D. *Alloy Carbide Precipitation at α:γ Boundaries*

Hackenberg and Shiflet[66] have proposed that alloy carbide precipitation at α:γ boundaries is responsible for incomplete transformation as well as the bay in the TTT curve for the initiation of transformation. Although they have established that X diffusion into such carbides can take place along the α:γ boundaries as well as through both austenite and ferrite, the volume diffusion involved, particularly through austenite, should quickly halt transformation, with subsequent resumption not to be anticipated.

Reynolds *et al.*[14] have shown that incomplete transformation in Fe-C-Mo alloys is associated with the *absence* of Mo_2C precipitation at α:γ boundaries. The termination of the stasis interval occurs in the *presence* of Mo_2C precipitation at these boundaries. A similar situation was observed in a Fe-0.13 pct C-2.99 pct Cr alloy.[20]

E. *Coupled Solute Drag Effect Theories*

A solute drag-type effect was proposed[12,67,68] as an explanation for slower than expected ferrite allotriomorph growth kinetics at temperatures below that of the upper nose of the ferrite-start TTT curve in an Fe-C-Mo alloy.[12] This effect is now described as a ''coupled solute drag effect,'' *i.e.,* a C-SDE.[24] Coupling occurs because accumulation of X at mobile areas of α:γ boundaries reduces the carbon concentration in these areas while the altered carbon concentration simultaneously changes the X concentration.[22] The reduction in carbon concentration reduction at these boundaries reduces growth kinetics. When this carbon concentration, or more accurately the chemical potential of carbon in austenite at mobile areas of α:γ boundaries, is reduced to that of the carbon concentration in regions remote from these boundaries, growth will stop,[14,23] thereby yielding ''growth stasis.''[23] In order that ''transformation stasis'' may occur, it is necessary that ferrite nucleation at austenite grain boundaries[22] and at α:γ boundaries (sympathetic nucleation)[14] should both cease, *i.e.,* that ''nucleation stasis'' must also develop.

1. *A further developed version of C-SDE–based explanation[13,22,23] for growth stasis*

An aspect of growth stasis that has not been considered in much detail is that the driving force for growth is reduced not only by the overlap of the carbon diffusion fields associated with adjacent ferrite precipitates but also, following Purdy and Brechet,[22] by the expansion of the carbon diffusion field associated with the growth of even a completely isolated ferrite crystal. Hence, the drag force needed to overcome the driving force for growth will be significantly reduced at later reaction times. Inasmuch as the nucleation rate is a function of the exponential of the square of the driving force for nucleation, even a small amount of diffusion field overlap should drastically reduce the nucleation kinetics of grain boundary ferrite allotriomorphs.

2. *C-SDE plus transition from PE to LE-NP to local equilibrium–partition as an explanation for growth stasis*

During the present symposium, much emphasis has been placed upon growth under local equilibrium–no partition (LE-NP) rather than under PE conditions. The ferrite allotriomorphs thickening kinetics data of Kinsman and Aaronson[24] and of Bradley and Aaronson[25] on various Fe-C-X alloys (where X was Al, Si, Ni, Mn, Co, and Cr) were interpreted on the basis of PE kinetics because the maximum penetration distance of X into austenite during the longest isothermal reaction time used was less than one austenite lattice parameter except at particularly high reaction temperatures. The Bradley–Aaronson[25] data were consistent with LE-NP kinetics only when they were similar to those for PE boundary conditions. Oi *et al.*[28] used a conventional isothermal transformation technique and

differential thermal analysis techniques to study ferrite growth kinetics in Fe-C-Mn and Fe-C-Ni alloys. Their experimentally determined outer limits for unpartitioned growth were shown to fall at or outside the calculated limit for NP-LE growth, though well within the region for PE growth. Recently, Purdy *et al.*[69] studied ferrite growth kinetics in Fe-C-Ni alloys during decarburization. These kinetics matched those of LE-NP, rather than of PE, at all times and temperatures studied. These results were the reverse of those reported by Bradley and Aaronson[25] for Fe-C-Ni alloys with higher Ni concentrations. Purdy *et al.*[69] pointed out, however, that their technique is inaccurate at short reaction times. Bradley and Aaronson[25] measured allotriomorph thickening kinetics, using conventional isothermal transformation techniques (which can be accurate after reaction times of a few seconds), at reaction times up to 180 seconds at the highest reaction temperature (715 °C) in their Fe-0.12 pct C-3.28 pct Ni but up to only 49, 11, and 10 seconds, respectively, at three lower temperatures (down to 650 °C). In their Fe-0.43 pct C-7.51 pct Ni alloy, reaction times ranged from 10 minutes at their highest temperature (570 °C) to 1 minute at 530 °C, their lowest temperature. Figures 4 through 6 in Purdy *et al.*[69] indicate that a clear difference between the two growth models appeared only after 10 minutes in an Fe-0.50 pct C-0.97 pct Ni alloy decarburized at 775 °C and in an Fe-0.38 pct C-1.03 pct Ni alloy decarburized at 800 °C. Only in an Fe-0.50 pct C-1.66 pct Ni alloy decarburized at 775 °C was a distinction possible at <10 minutes. These differences between the results of the conventional isothermal transformation and the decarburization techniques can be reconciled on the view that ferrite formation in all of these experiments began with PE but transitioned to LE-NP at sufficiently long reaction times. (When phenomena such as ICT, which occurs at late stages of reaction, are being investigated and carbon diffusion field overlap is to be avoided, however, the decarburization technique is far superior because the austenite grain size is then effectively infinite.)

Bradley and Aaronson[25] discarded NP-LE growth as an explanation for their results because the maximum diffusion distance in austenite was appreciably less than one austenite lattice parameter under almost all circumstances studied. A similar situation prevails in the Oi *et al.*[28] data. Enomoto[70] has proposed during this symposium a mechanism through which the LE-NP mechanism can be made allowable, namely, that the diffusion of X needed to achieve LE-NP boundary conditions at $\alpha{:}\gamma$ boundaries takes place primarily through ferrite, in which the diffusivity of X at a given temperature is approximately 100-fold larger than in austenite. Ferrite would still have to nucleate in austenite, of course; this will occur mainly at austenite grain boundaries. However, the atomic movements during ferrite nucleation can take place by diffusion along austenite grain boundaries and $\alpha{:}\gamma$ boundaries.[71] During PE growth, the Ni concentration in ferrite is of course the same as that in austenite and in the bulk alloy prior to transformation. After the C-SDE and overlap of the carbon diffusion fields of adjacent ferrite crystals have slowed growth kinetics sufficiently, the diffusion of Ni from ferrite into austenite, driven by the high supersaturation of Ni in ferrite relative to that of the much lower concentration at equilibrium, can now take place. Although bulk diffusion of Ni into austenite is still not possible in the reaction time-temperature regions of Fe-C-Ni alloys investigated by Bradley and Aaronson,[25] Oi *et al.*,[28] and Purdy *et al.*,[69] once the LE-NP Ni concentration is achieved on the ferrite side of the $\alpha{:}\gamma$ boundary, the relatively high transboundary diffusivity should permit the counterpart Ni concentration to be achieved soon afterward in the first plane on the austenite side of the boundary, even though an appreciably longer time will be required for Ni diffusion to penetrate into the next plane in the austenite.

Bradley and Aaronson[25] have shown that LE-NP growth kinetics can be indistinguishable from PE growth kinetics in the ''no partition'' temperature-composition region. Extension of the LE analysis into the temperature region where bulk partition is found experimentally to take place, however, results in calculated growth kinetics orders of magnitude greater than those measured experimentally. Hackenberg and Shiflet[66] have suggested on the basis of another point of view that when partition of X between austenite and ferrite begins at temperatures characteristic of the bay in the ferrite-start curve in TTT diagrams, conversion of LE-NP to LE-P (local equilibrium–partition) should correspond to the onset of stasis. Humphreys *et al.*[24] have used scanning transmission electron microscopy (TEM) analysis to show that the Mo concentration at $\alpha{:}\gamma$ boundaries increases in the presence of stasis. However, their data encompassed a region 16-nm wide, centered about individual $\alpha{:}\gamma$ boundaries. Hence, these data must have reflected diffusion at least in the ferrite phase. In an accompanying article, Guo *et al.*[72] have used STEM analysis to demonstrate experimentally that in an Fe-0.04 pct C-3 pct Mn-2.9 pct Si alloy, Mn partition into austenite accompanies stasis. (The simultaneous presence of Mn and Si enhances the C-SDE.*)

*Si could not be reliably detected in these experiments. Inasmuch as the diffusivity of Mn is appreciably slower than that of Si at a given temperature in both phases,[72] however, the Mn data should have captured the essential features of the diffusional processes taking place in the vicinity of the $\alpha{:}\gamma$ boundaries.

These authors accordingly concluded that the transformation sequence is (1) PE; (2) with the aid of the strong C-SDE and carbon diffusion field overlap, growth kinetics of ferrite are markedly slowed or stopped; and (3) once Mn (and Si) diffusion in austenite begins at LE-NP, the interface is trapped and stasis begins. This summarizes the view adopted here when X partition between austenite and ferrite accompanies stasis.

3. *Hillert and co–workers' views on incomplete transformation and related topics*

In his article at the 1968 Manchester symposium on phase transformations, Hillert[67] considered the growth kinetics data of Kinsman and Aaronson[27] on an Fe-0.11 pct C-1.1 pct Mo alloy in which the parabolic rate constant for allotriomorph thickening passed through a maximum at the temperature of the upper nose of the ferrite-start TTT curve. He also concluded, after examining various possibilities, that a solute draglike effect was responsible.

Recently, Hillert[73] considerably elaborated on this approach. He proposed that bainite consists of Widmanstätten ferrite with or without carbides, *i.e.,* he accepted the

''surface relief'' definition of bainite.[4] In Fe-C alloys, the upper temperature limit of Widmanstätten ferrite formation was found to lie appreciably above the T_o *vs* pct C and the T_o' *vs* pct C curves (where T_o' is the T_o temperature corrected for transformation strain energy). In unpublished work,[74] the energy barrier for sideplate formation was evaluated and denoted as Δ_{FeC}, the driving force for ferrite sideplate formation at the reaction temperature where sideplates first appear at a given pct C in Fe-C alloys. This is described as the W_s temperature.[21] In Fe-C-X alloys, it was found necessary to add an additional energy barrier, Δ_X, because of the change in the W_s induced by the alloying element addition. The Δ_X was attributed to a solute drag effect. These energy barriers were added to the Gibbs energy of the growing ferrite.

Focusing upon Δ_{Mo}, the carbon content of the untransformed austenite during incomplete transformation in Fe-0.064 pct C-1.80 pct Mo and Fe-0.19 pct C-1.81 pct Mo was calculated (as in Section IV–B–1–c) as a function of isothermal reaction temperature from the data of Reynolds *et al.*[14] The Δ_{Mo} was added to Δ_{FeC} to calculate the displacement of the PE Ae_3 curve to the carbon content of the untransformed austenite, as shown in Figure 14.[73] This displacement reduces the supersaturation for Widmanstätten ferrite formation to zero at the temperature and carbon concentration corresponding to the C curve for the initiation of the ORK bainite reaction. The dashed vertical line in this figure is seen to intersect the 1.80 pct Mo curve at three points. The W_s temperature at this pct C and pct Mo is designated by the first intersection. The second intersection represents the lower temperature limit of the Widmanstätten ferrite region. The B_s temperature is represented by the third intersection. No Widmanstätten structure should form between the second and third intersections. In an Fe-0.10 pct C-Fe-2.70 pct Mo alloy, there will be no acicular ferrite; only bainitic structures will appear. Using the Mo-modified Ae_3 curves in Figure 14 and an early version of the Zener[5]–Hillert[75] equation, Figure 15[73] plots C curves for the lengthening rate of Widmanstätten ferrite and bainite in Fe-C-1.80 pct Mo alloys in the presence of the bulk carbon concentrations labeled on the various C curves. For simplicity, the Wagner[76] approximation was used, *i.e.,* assuming that the diffusivity of carbon in austenite (which varies markedly with composition, particularly at high carbon concentrations[78]) is that corresponding to the interface composition. At reaction temperatures below that of the B_s curve in Figure 14, the formation of Widmanstätten bainite plates should cease when the average carbon concentration in the remaining austenite reaches this curve. (Note that this arrangement is not applicable to Widmanstätten ferrite plates.) This permits the proportion of ferrite present at stasis to be calculated, as shown in Figure 16.[73] Thus, a quantitative accounting is made for the incomplete transformation phenomenon.

Hillert concluded that the growth of grain boundary allotriomorphs is less retarded by Mo than is that of Widmanstätten ferrite. He ascribes this difference to the presence of carbides within the allotriomorphs that drain Mo from α:γ boundaries. However, carbides are essentially absent from degenerate ferrite formed below the bay temperature where retardation of ferrite growth can be sufficient to produce incomplete transformation in Fe-C-Mo[14] and Fe-C-Cr[15] alloys. His emphasis on continuity of ferrite and (overall reaction kinetics) bainite is in accord with the present authors' and related writings.[68,77–79]

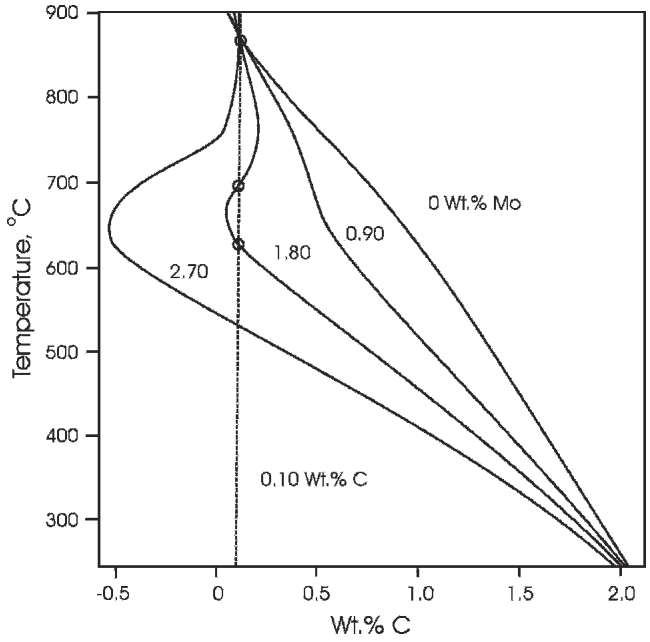

Fig. 14—PE Ae_3 curve shifted when the free energy of ferrite is increased by $\Delta_{FeC} + \Delta_{Mo}$ for indicated pct Mo on the various curves.[73]

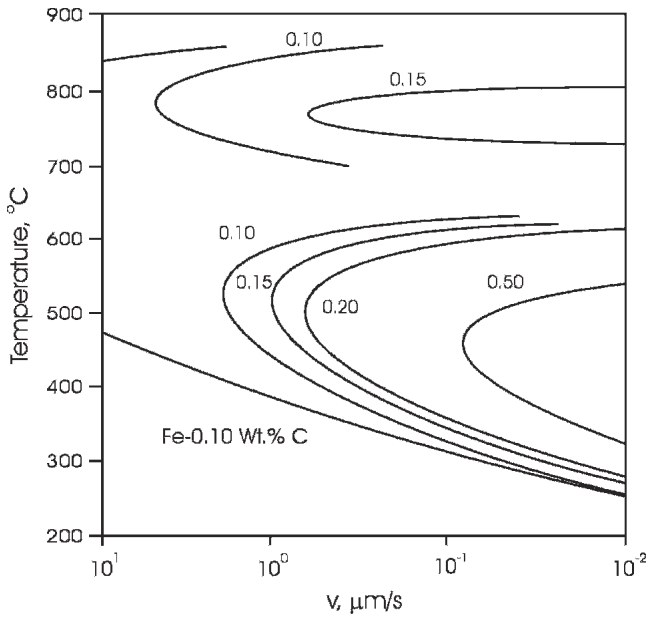

Fig. 15—Calculated lengthening rate of acicular ferrite in Fe-pct C-1.80 pct Mo alloys for the indicated wt pct C; also for an Fe-0.10 pct C alloy.[73]

With the aid of Δ_{Mo} values obtained from experiment-based data on the carbon content of the untransformed austenite during stasis in Fe-C-Mo alloys, Hillert was thus able to assess the reduction in the bulk carbon concentration needed to produce incomplete transformation. This achievement represents an important advance in our understanding of the incomplete transformation phenomenon. As previously noted, however, transformation stasis requires

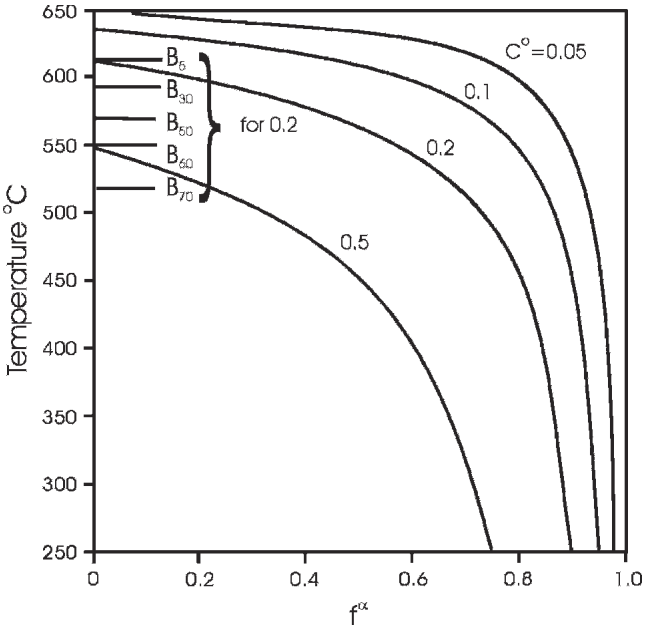

Fig. 16—The final fraction of acicular ferrite, f^{α}, as a function of reaction temperature for Fe-wt pct C-1.80 pct Mo alloys, with the wt pct C (C^{o}) indicated on each curve. The B_{pct} values indicated by short parallel lines perpendicular to the temperature axis indicate the temperature at which transformation ceases after the pct ferrite noted in the subscript has formed in an Fe-0.2 pct C-1.80 pct Mo alloy; B_s corresponds to $f^{\alpha} = 0$.[73]

not only growth stasis but also nucleation stasis. This factor considerably complicates analysis of incomplete transformation.

V. DISCUSSION

A. *Role of Nucleation Kinetics in ICT*

Nucleation stasis involves the cessation of nucleation at two different types of site: austenite grain boundaries and austenite:ferrite boundaries (sympathetic nucleation). Consider first ferrite nucleation at austenite grain boundaries. Measurements of the steady-state nucleation rate (J_s^*) of ferrite allotriomorphs at austenite grain boundaries at temperatures from above the nose of the ferrite-start TTT curve down to the bay in this curve in an Fe-0.18 pct C-4.25 pct Mo alloy have shown that the nucleation rate *vs* reaction temperature curve is roughly parallel to the ferrite-start TTT curve.[26] (Severe degeneracy of the ferrite prevented nucleation rate measurements at temperatures below that of the bay in this alloy.[29]) Analysis of J_s^* data in Fe-C-X alloys (where X = Mn, Mo, Ni, Si, and Co) indicated that the critical nuclei of orthoequilibrium (*i.e.,* full ternary equilibrium) composition achieved by volume diffusion of X in austenite is the most likely among several mechanisms considered. This leads to the obvious Hultgren[29]-type suggestion that at reaction temperatures below that of the bay the critical nuclei will be of PE composition. A clear distinction between the foregoing mechanism and that of PE with carbon diffusion control could not be made from the available data. This problem is further considered in Section B in the context of ferrite growth in Fe-C-Mn alloys.

A combination of Auger electron spectroscopy measurements of alloying element concentrations at former austenite grain boundaries and application of the Guttmann–McLean[80] analysis to these results indicates that Mo has an exceptionally strong tendency to segregate to austenite grain boundaries and thus to reduce the average austenite grain boundary energy.[81] No direct measurements have as yet been made of alloying element effects on α:γ boundary energy. It appears that individual alloying elements do not exert accurately parallel effects upon austenite grain boundary and α:γ boundary energy.[29] The possibility remains open, however, that the low nucleation rates found at the bay temperature may have resulted primarily from the particularly low austenite grain boundary energy at this temperature in the Fe-C-Mo alloy studied. The possibility is further bruited that the apparently very rapid increase in nucleation kinetics at sub-bay temperatures arises primarily from a rapid increase in sympathetic nucleation kinetics rather than nucleation at grain boundaries.

B. *Tests of C-SDE* vs *LE-NP Theories of ICT*

Following Purdy *et al.*,[82] if X is an austenite stabilizer such as Mn or Ni and the alloy composition lies in the LE-P region and above the ''zero-partition'' boundary, growth must be accompanied by partition of X from ferrite into austenite, whereas if X is a ferrite stabilizer, diffusion of X into ferrite is required (Figure 17). Below the zero partition boundary in Figure 17, only carbon diffusion in austenite is needed *after* highly localized partition of X between the two phases in order to establish local equilibrium with respect to X and carbon at mobile areas of the α:γ boundaries. These sequences of precipitation assume that all volumes of ferrite are in diffusional communication with untransformed austenite regions in which the ''bulk'' carbon concentration of carbon in austenite is the same as that in the alloy. Once there is sufficient overlap of carbon diffusion fields associated with ferrite so that the bulk carbon composition shifts laterally, *i.e.,* parallel to the carbon concentration axis, Figure 17 shows that in the most carbon-enriched regions, transformation could shift from PE → PE/LE-NP → PE/LE-P → LE-P. Given the still significant difficulties associated with determining experimentally the carbon concentration in micron-sized volumes of a steel thin foil, the most practical method for ascertaining whether the original bulk carbon concentration has been exceeded is to measure the thickening kinetics of grain boundary ferrite allotriomorphs in specimens austenitized so that nearly all austenite grain boundaries are about perpendicular to the intended plane of polish. If this is done by plotting the thickness of the thickest grain boundary allotriomorph as a function of the square root of the isothermal reaction time, the boundary condition that the bulk carbon concentration be retained during growth must be considered to have been violated if data points fall significantly below the maximum thickness *vs* (growth time)$^{1/2}$ correlation line.[83,84] Thickness data taken at reaction times where this correlation is violated must thus be discarded. In Section IV–E–2, the conclusion that conventional isothermal transformation studies had demonstrated that PE was initially present in Fe-C-Ni alloys[25] appeared to contradict the finding that LE-NP was operative throughout carburization/decarburization studies in Fe-C-Ni

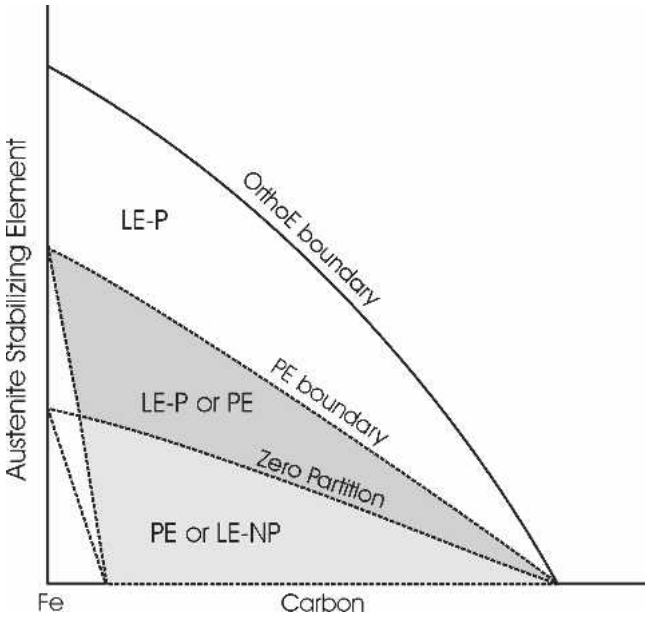

Fig. 17—Isothermal wt pct X (austenite-stabilizing alloying element) *vs* wt pct C section showing regions in which only Le-P, LE-P or PE (PE), or PE or LE-NP can be present. The orthoequilibrium (OE) boundary is the full equilibrium (with respect to both C and Mo) $\alpha + \gamma$ boundary.[28]

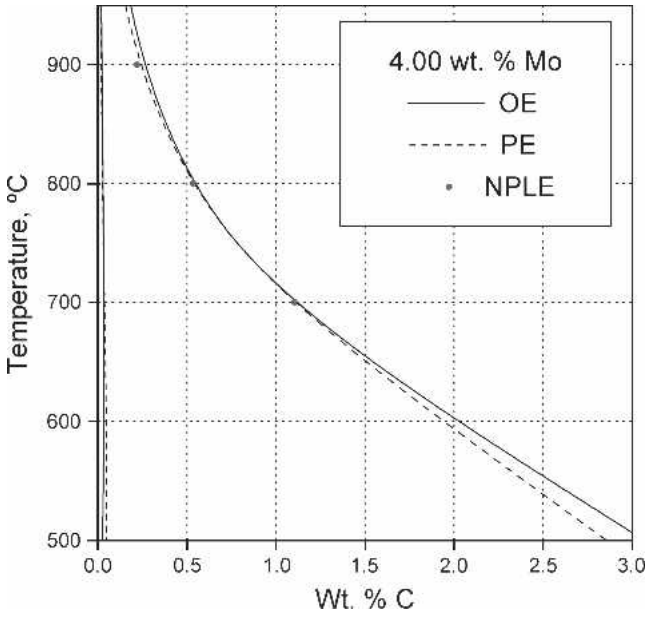

Fig. 18—OE, PE, and NP-LE computed from Thermo-Calc for Fe-C-1.95 pct Mo alloys.

alloys was traced to the ability of this technique to study reproducibly ferrite growth kinetics only after reaction times at which the PE → LE-NP transition had already taken place.

Figures 18(a) through (c) show the orthoequilibrium and PE $\gamma/(\alpha + \gamma)$ phase boundaries and calculated data points for the NP-LE phase boundary for Fe-C-2.95 pct Mo, the Fe-C-1.95 pct Mo, and the Fe-C-4.00 pct Mo alloys, respectively. These boundaries were computed with Thermo-Calc. The differences among these boundaries are clearly so small that they cannot be used to determine the type of partition mechanism operative. The circumstance that the equilibrium tie-lines in the $\alpha + \gamma$ region are nearly parallel to the wt/pct C axis is basically responsible for this outcome.[85]

C. *Consideration of Generalizations (Section II) on ICT Based on C-SDE– and Partition-Based Theories*

1. *IC Transformation Is Not a Generally Occurring Phenomenon in Fe-C-X Alloys[14,19]*

(C-SDE) On our present views, when the binding energy of X to α:γ boundaries is small, the C-SDE will be too small to permit ferrite growth to be halted in the PE region.

(Partition) When the alloy composition and the range of reaction temperatures are such that they lie below the ''no partition'' curve, ICT is not feasible.

2. *A bay in the TTT curve for the beginning of transformation in a given Fe-C-X alloy does not necessarily mean that ICT occurs in this alloy[14]*

(C-SDE) A bay in the ferrite-start TTT curve can be produced when the pct C, pct X, and the resulting strength of the C-SDE are too small to permit development of ICT at any reaction temperature but suffice to slow growth kinetics at intermediate temperatures enough to produce a bay in the ferrite-start TTT curve.[14]

(Partition) This observation cannot be explained straightforwardly on a ''partition'' basis. Breaching the no partition boundary should cause ICT, whereas failure to do so cannot explain a bay in the ferrite-start TTT curve.

3. *ICT occurs over a wider temperature range at a given pct X with increasing pct C[14] and at a given pct C with increasing pct X[14]*

(C-SDE) The driving force for ferrite growth at a given reaction temperature decreases with increasing carbon concentration. If a C-SDE is operative, this effect will accordingly be strengthened as the bulk carbon concentration in the alloy is increased because the driving force for growth will be decreased. Similarly, the C-SDE will increase as the bulk concentration of X in the alloy is increased.

(Partition) This approach explains an increasing tendency toward ICT with increasing pct C and pct X because the bulk chemistry of the alloy will approach the no partition boundary.

4. *At a given pct C, ICT appears to occur over a wider temperature range as $\varepsilon_{12}^{\gamma}$* becomes increasingly negative and again but much more slowly when $\varepsilon_{12}^{\gamma} > 1$; when $\varepsilon_{12}^{\gamma}$ is similar for two X's, the one having a larger size difference with respect to Fe will have the stronger effect[13]*

*$\varepsilon_{12}^{\gamma}$ is the Wagner interaction parameter, 1 represents C and 2 denotes X.

(C-SDE) Making the Wagner interaction parameter $\varepsilon_{12}^{\gamma}$ increasingly positive sets a rough upper limit on the C-SDE that is reached when there are, on average, no C atoms nearest neighboring to an *X* atom in the vicinity of α:γ boundaries.[13] However, when $\varepsilon_{12}^{\gamma}$ is increasingly negative, carbon atoms can continue to be added to successive *n*th nearest neighboring shells and thereby strengthen the C-SDE, albeit at a decreasing rate for successive shells.

(Partition): Not relevant.

5. *Carbide precipitation does not occur at α:γ boundaries during stasis[14,15]*

(C-SDE) Stasis is associated with sympathetic nucleation of ferrite[43,86] at α:γ boundaries.[14] Despite the disadvantage with respect to the driving force for nucleation, the sympathetic nucleation kinetics are self-evidently more rapid than are alloy carbide nucleation kinetics at α:γ boundaries. The binding energy of Mo to α:γ boundaries appears to increase with decreasing isothermal reaction temperature.[87] This finding suggests that the energy of the partly coherent α:γ boundaries at which sympathetic nucleation takes place decreases at lower temperatures, thereby making them less favorable sites for sympathetic nucleation provided that ferrite:alloy carbide boundaries are not similarly or still further decreased in interfacial energy.

(Partition) Not relevant.

6. *Twin boundary ferrite occurs preferentially in the bay region when $\varepsilon_{12}^{\gamma}$ is appreciably <1[36,37]*

(C-SDE and Partition): As recently discussed, this effect does not appear to be directly associated with either the C-SDE or with X partition between austenite and ferrite.[13] However, Brown *et al.*[37] have observed high densities of incoherent twin boundaries in an Fe-C-Mo alloy studied at 900 °C with high-voltage, high-temperature TEM. Such sites should be particularly favored as nucleation sites for ferrite allotriomorphs.[13,37] Possibly, Mo and Cr increase the probability of incoherent twin boundary formation by reducing the energy of such interfaces through clustering of carbon atoms around Mo atoms associated with them.

7. *"Wrinkled ferrite"[36,37] formation also occurs preferentially in the bay region when $\varepsilon_{12}^{\gamma}$ is appreciably <1[13]*

(C-SDE and Partition): The connection between these phenomena and the C-SDE is not obvious. There also does not appear to be a clear connection between them and X partition between austenite and ferrite. The key to the development of this microstructure is probably the formation of many dislocations in ferrite in contact with α:γ boundaries.[37] The volume change associated with ferrite formation is probably larger in Fe-C-X alloys when X = Mo than when X = Cr, as indicated by the much larger lattice parameter difference between Fe and Mo than between Fe and Cr.[12] This suggests that "wrinkled ferrite" may be more prominent when X = Cr than when X = Mo, though this point has yet to be tested. However, the carbides associated with ferrite are different in Fe-C-Cr[20] than in Fe-C-Mo[33] alloys, thereby making this experiment less critical in character. The difference in bay temperatures in the two systems should also have an effect upon dislocation production.

D. *Where Do We Go from Here?*

1. *General remarks*

As indicated in this and in a preceding article,[13] the quantitative literature on ICT in Fe-C-X alloys is largely devoted to Fe-C-Mo alloys. Publications on this subject for other Fe-C-X systems are too often complicated by the presence of more than trace concentrations of other X's, fine austenite grain sizes, transformation during continuous cooling rather than isothermally, and determination of the fraction of austenite transformed by indirect methods (*e.g.,* dilatometry) of questionable reliability rather than by quantitative metallography. Further, surveys of the principal microconstituents present and their often intricate details with optical microscopy as a function of isothermal reaction temperature, pct C and pct X, are also too limited when X is not Mo. Obviously, the classical optical microscopy observations must now be heavily supplemented with scanning electron microscopy (SEM) observations conducted over wide ranges of magnifications. The value of this information presently available is also reduced by the absence of information obtained over a range of carbon concentrations and of X concentrations, data on nucleation kinetics, measurements of the thickening kinetics of grain boundary allotriomorphs or the lengthening kinetics of sideplates, information permitting determination as to whether such measurements were made in the presence of significant diffusion field overlap by nearby ferrite crystals, and TEM observations on carbide distribution at α:γ boundaries. Supply of such information, particularly when X = Cr, Mn, Ni, Si, and Cu, would be of particular value. Although this program calls for a large amount of experimental research, this might be accomplished by international collaboration among many laboratories, provided that a single source of alloys is used for a given Fe-C-X system—and, ideally, for all Fe-C-X systems studied. As many of the very large number of heat treatments needed as is possible should also be conducted at a single laboratory. Microscopy observations, particularly with optical microscopy and SEM, on the other hand, might be shared among many laboratories. Good communication among participants is also very important. Continuation of the symposium series on ferrite formation in Fe-C-X alloys[91] (of which the fourth was held in conjunction with the Hillert 80th birthday symposium at which this paper was presented) would be an appropriate method of ensuring such communication, particularly if the proceedings of each were to be published mainly in this journal.

2. *A specific proposal*

The Fe-C-X system that now seems to be most appropriate for critical studies on ICT is Fe-C-Mn. Much more than in the case Fe-C-Mo, there is extensive, primarily theoretical information[88] available on the various LE boundaries in this system as well as more experimental data on these boundaries than in any other Fe-C-X system.[88] Unlike the case of Fe-C-Mo (Figure 18), the LE boundaries in Fe-C-Mn are well separated.[88] There is already some growth kinetics data available in Fe-C-Mn alloys.[25,28] Because of these advantages, the Fe-C-Mn system might well be the most appropriate one in which to conduct the more wide ranging studies described in Section V–D–1.

VI. CONCLUSIONS

1. The ICT phenomenon consists of the cessation of transformation of austenite to ferrite at a fraction transformed significantly less than that allowed by application of the Lever rule to the phase boundaries of the $\alpha + \gamma$ region or its metastable equilibrium extrapolation to temperatures

below that of the eutectoid.[2] This phenomenon is the central component of the "overall reaction kinetics" definition of bainite but can be irrelevant to both the generalized microstructural and the surface relief definitions of bainite.[12,19]

2. Experimentally observed generalizations made on the ICT phenomenon and the relative strength of the C-SDE required to produce the ICT as compared with many other alloying element effects upon ferrite formation in Fe-C-X alloys have been briefly summarized upon the basis of a recent detailed review.[13]
3. Explanations or theories of the ICT transformation that have been offered in the literature are summarized and critiqued (markedly extending previous considerations on this topic[13]). Explanations shown to be basically unsatisfactory include the following: (a) the ICT is absent only when superceded by the pearlite reaction;[3] (b) the plate- or lath-shaped ferritic component of bainite forms by shear taking place at much higher velocities than those allowed by carbon diffusion control;[7,8] (c) individual subunits comprising sheaves grow by high velocity shear, with appreciable delays between successive shears[42] such as will allow carbon diffusion-controlled lengthening kinetics to be simulated; (4) in between high velocity shears, carbon diffuses from the initially more or less fully supersaturated ferrite plates into the surrounding austenite until the carbon concentration of the austenite reaches the T_o composition, whereupon ICT commences;[44] (5) growth of bainite plates can occur by diffusion-controlled shear;[50,51] (6) transformation strain energy release can account for the characteristics of ICT;[59,60] and (7) alloy carbide precipitation at α:γ boundaries can explain ICT.[66]
4. Theories that provide promising explanations for the ICT include the following: (1) the C-SDE can be strong enough under appropriate thermodynamic and kinetics circumstances to halt carbon diffusion-controlled PE growth; and (2) the C-SDE and overlap of carbon diffusion fields associated with nearby ferrite crystals lead successively from PE to LE-NP and finally to LE-P at much earlier stages of ferrite formation and at smaller carbon and X concentrations and wider ranges of reaction temperature than would be feasible without the assistance of the C-SDE and carbon diffusion field overlap.[72]
5. The suggestion is offered that future experimentally based isothermal transformation studies on the ICT be focused upon Fe-C-Mn rather than on Fe-C-Mo alloys. Although the C-SDE is obviously much more powerful in Fe-C-Mo alloys, Thermo-Calc–based computations made during the current study have shown that the LE-NP, PE, and the ortho-equilibrium boundaries nearly coincide in Fe-C-Mo alloys, whereas in Fe-C-Mn alloys, they are known to be adequately separated.[28,82] Appreciably higher Mn concentrations will probably be required than those used in Fe-C-Mo alloys in order to produce equivalent strength of counterpart effects upon ferrite formation.[28]

ACKNOWLEDGMENTS

The authors are grateful to Dr. Dmitri Malakhov for assistance with the computational thermodynamics underlying Figures 6 and 18. One of the authors (GRP) acknowledges the support of the Natural Sciences and Engineering Research Council of Canada.

REFERENCES

1. F. Wever and E. Lange: *Eisenforsch*, 1932, vol. 14, p. 71.
2. R.F. Hehemann, K.R. Kinsman, and H.I. Aaronson: *Metall. Trans.*, 1972, vol. 3, p. 1077.
3. R.F. Hehemann and A.R. Troiano: *Met. Progr.*, 1956, vol. 70 (2), p. 97.
4. H.I. Aaronson, W.T. Reynolds, Jr., G.J. Shiflet, and G. Spanos: *Metall. Trans. A*, 1990, vol. 21A, p. 1343.
5. C. Zener: *Trans. AIME*, 1946, vol. 167, p. 550.
6. H.I. Aaronson, G.R. Purdy, D.V. Malakhov, and W.T. Reynolds, Jr.: *Scripta Mater.*, 2001, vol. 44, p. 2425.
7. J.M. Robertson: *J. Iron Steel Inst.*, 1929, vol. 11, p. 391.
8. E.S. Davenport and E.C. Bain: *Trans. AIME*, 1930, vol. 90, p. 117.
9. H.J. Lee, G. Spanos, G.J. Shiflet, and H.I. Aaronson: *Acta Metall.*, 1988, vol. 36, p. 1129.
10. J.W. Christian and D.V. Edmonds: *Phase Transformations in Ferrous Alloys*, TMS, Warrendale, PA, 1984, p. 293.
11. H.I. Aaronson and W.T. Reynolds, Jr.: *Scripta Metall.*, 1988, vol. 22, p. 567.
12. P.G. Boswell, K.R. Kinsman, G.J. Shiflet, and H.I. Aaronson: *Mechanical Properties and Phase Transformations in Engineering Materials*, TMS, Warrendale, PA, 1986, p. 445.
13. H.I. Aaronson, W.T. Reynolds, Jr., and G.R. Purdy: *Metall. Mater. Trans. A*, 2004, vol. 35A, p. 1187.
14. W.T. Reynolds, Jr., F.Z. Li, C.K. Shui, and H.I. Aaronson: *Metall. Mater. Trans. A*, 1990, vol. 21A, p. 1433.
15. T. Lyman and A.R. Troiano: *Trans. ASM*, 1946, vol. 37, p. 402.
16. J.V. Russell and F.T. McGuire: *Trans. ASM*, 1944, vol. 33, p. 103.
17. G. Papadimitriou and J.M.R. Genin: *Phase Transformations in Solids*, North-Holland, New York, NY, 1984, p. 747.
18. J.P. Sheehan, C.A. Julien, and A.R. Troiano: *Trans. ASM*, 1949, vol. 41, p. 1165.
19. W.T. Reynolds, Jr., S.K. Liu, F.Z. Li, S. Hartfield, and H.I. Aaronson: *Metall. Trans. A*, 1990, vol. 21A, p. 1479.
20. H. Goldenstein and H.I. Aaronson: *Metall. Trans. A*, 1990, vol. 21A, p. 1465.
21. H.I. Aaronson, P.G. Boswell, and K.R. Kinsman: *Mechanical Properties and Phase Transformations in Engineering Materials—Earl R. Parker Symp. on Structure Property Relationships*, TMS-AIME, Warrendale, PA, 1986, p. 467.
22. G.R. Purdy and Y.M. Brechet: *Acta Mater.*, 1995, vol. 43, p. 3763.
23. G.J. Shiflet and H.I. Aaronson: *Metall. Trans. A*, 1990, vol. 21A, p. 1413.
24. E.S. Humphreys, H.A. Fletcher, J.D. Hutchins, A.J. Garratt-Reed, W.T. Reynolds, Jr., H.I. Aaronson, G.R. Purdy, and G.D.W. Smith: *Metall. Mater. Trans. A*, 2004, vol. 35A, p. 1223.
25. J.R. Bradley and H.I. Aaronson: *Metall. Trans. A*, 1981, vol. 12A, p. 1729.
26. T. Abe, H.I. Aaronson, and G.J. Shiflet: *Metall. Trans. A*, 1985, vol. 16A, p. 521.
27. K.R. Kinsman and H.I. Aaronson: *Transformation and Hardenability in Steels*, Climax Molybdenum Co., Ann Arbor, MI, 1967, p. 39.
28. K. Oi, C. Lux, and G.R. Purdy: *Acta Mater.*, 2000, vol. 48, p. 2147.
29. M. Enomoto and H.I. Aaronson: *Metall. Trans. A*, 1986, vol. 17A, p. 1385.
30. N.F. Kennon and N.F. Kaye: *Metall. Mater. Trans. A*, 1982, vol. 13A, p. 975.
31. H.I. Aaronson and H.A. Domian: *Trans. TMS-AIME*, 1966, vol. 236, p. 781.
32. A. Hultgren: *Trans. ASM*, 1947, vol. 39, p. 915.
33. H. Tsubakino and H.I. Aaronson: *Metall. Trans. A*, 1987, vol. 18A, p. 2047.
34. R.E. Hackenberg, D.P. Nørdstrom, and G.J. Shiflet: *Scripta Mater.*, 2002, vol. 47, pp. 357-61.
35. K.M. Wu, M. Kagayama, and M. Enomoto: *Mater. Sci. Eng.*, 2002, vol. A343, p. 143.
36. A. Hultgren: *Kungl. Svenska Vet. Akad. Handl.*, 1953, vol. 4, p. 3.
37. R.B. Brown, H. Badekas, and G.R. Purdy: *Metallography*, 1983, vol. 16, p. 375.
38. M. Hillert: Internal Report, Swedish Institute for Metals Research, Stockholm, 1960.

39. M. Hillert: *Metall. Trans. A*, 1975, vol. 6A, p. 5.
40. M. Hillert: *Scripta Mater.*, 2002, vol. 47, p. 181.
41. T. Moritani, N. Miyajima, T. Furuhara, and T. Maki: *Scripta Mater.*, 2002, vol. 47, p. 193.
42. J.M. Oblak and R.F. Hehemann: *Transformation and Hardenability in Steels*, Climax Molybdenum Co., Ann Arbor, MI, 1967, p. 15.
43. H.I. Aaronson and C. Wells: *Trans. AIME*, 1956, vol. 206, p. 1216.
44. H.K.D.H. Bhadeshia and D. Edmonds: *Acta Metall.*, 1980, vol. 28, p. 1265.
45. H.I. Aaronson, W.T. Reynolds, Jr., G.J. Shiflet, and G. Spanos: *Metall. Trans. A*, 1990, vol. 21A, p. 1369.
46. H.K.D.H. Bhadeshia and D.V. Edmonds: *Metall. Trans. A*, 1979, vol. 10, p. 895.
47. E. Girault, P. Jacques, P. Ratchev, J. Van Humbeeck, B. Verlinden, and E. Aernoudt: *Mater. Sci. Eng.*, 1999, vols. A273–A275, p. 471.
48. P. Jacques, E. Girault, T. Catlin, T. Jop, S. van der Zwaag, and F. Delanney: *Mater. Sci. Eng.*, 1999, vols. A273–A275, p. 475.
49. A. Kutsov, Y. Taran, K. Uzlov, A Kimmel, and M. Evsyukov: *Mater. Sci. Eng.*, 1999, vols. A273–A275, p. 480.
50. T. Ko and S.L.A. Cottrell: *J. Iron Steel, Inst.*, 1952, vol. 172, p. 307.
51. T. Ko: *J. Iron Steel Inst.*, 1953, vol. 175, p. 16.
52. K.R. Kinsman, E. Eichen, and H.I. Aaronson: *Metall. Trans. A*, 1975, vol. 6A, p. 303.
53. J.M. Rigsbee and H.I. Aaronson: *Acta Mater.*, 1979, vol. 27, p. 365.
54. J.M. Rigsbee and H.I. Aaronson: *Acta Mater.*, 1969, vol. 27, p. 351.
55. C. Li, V. Perovic, and G.R. Purdy: *Phase Transformations '87*, Institute of Metals, London, 1988, p. 326.
56. T. Moritani, N. Miyajima, T. Furuhara, and T. Maki: *Scripta Mater.*, 2002, vol. 47, p. 193.
57. B.P.J. Sandvik and C.M. Wayman: *Metall. Trans. A*, 1983, vol. 14A, pp. 823 and 835.
58. G.R. Speich and M. Cohen: *Trans. AIME*, 1960, vol. 218, pp. 1050-59.
59. O. Bouaziz, D. Quidort, and P. Maugis: *Rev. Metall.-CIT*, 2003, vol. 1, p. 103.
60. D. Quidort, O. Bouaziz, and Y. Brechet: in *Austenite Formation and Decomposition*, E. Buddy Damm and M.J. Merwin, eds., TMS, Warrendale, PA, 2003, p. 15.
61. M.G. Hall and H.I. Aaronson: *Metall. Mater. Trans. A*, 1994, vol. 25A, p. 1923.
62. G.R. Speich: *Decomposition of Austenite by Diffusional Processes*, Interscience Publishers, New York, NY, 1962, p. 353.
63. J.D. Watson and P.G. MacDougall: *Acta Mater.*, 1973, vol. 21, p. 961.
64. J.P. Hirth, G. Spanos, M.G. Hall, and H.I. Aaronson: *Acta Mater.*, 1998, vol. 46, p. 857.
65. J.D. Eshelby: *Proc. R. Soc. A*, 1957, vol. 241, p. 376.
66. R.E. Hackenberg and G.J. Shiflet: in *Austenite Formation and Decomposition*, E. Buddy Damm and M.J. Merwin, eds., TMS, Warrendale, PA, 2003, p. 27.
67. M. Hillert: *The Mechanism of Phase Transformations in Crystalline Solids*, Institute of Metals, London. 1969, p. 231.
68. H.I. Aaronson: *The Mechanism of Phase Transformations in Crystalline Solids*, Institute of Metals, London. 1969, p. 270.
69. A. Phillion, H.S. Zurob, C.R. Hutchinson, H. Guo, D.V. Malakhov, J. Nakano, and G.R. Purdy: *Metall. Mater. Trans. A*, 2004, vol. 35A, p. 1237.
70. M. Enomoto: *Metall. Mater. Trans. A*, 2006, vol. 37A, pp. 1703-10.
71. G. Vander Velde, J.A. Velasco, K.C. Russell, and H.I. Aaronson: *Metall. Trans. A*, 1976, vol. 7A, p. 1472.
72. H. Guo, H.I. Aaronson, M. Enomoto, and G.R. Purdy: *Metall. Mater. Trans. A*, 2006, vol. 37A, pp. 1721-29.
73. M. Hillert and L. Höglund: in *Austenite Formation and Decomposition*, E. Buddy Damm and M.J. Merwin, eds., TMS, Warrendale, PA, 2003, p. 3.
74. M. Hillert, L. Höglund, and J. Agren: Royal Institute of Technology, Stockholm, unpublished research, 2005.
75. M. Hillert: *Jernkon. Annal.*, 1957, vol. 141, p. 757.
76. C. Wagner: *Trans. AIME*, 1952, vol. 194, p. 91.
77. H.I. Aaronson and C. Wells: *Trans. AIME*, 1955, vol. 203, p. 1002.
78. L. Kaufman, S.V. Radcliffe, and M. Cohen: *Decomposition of Austenite by Diffusional Processes*, Interscience, New York, NY, 1962, p. 313.
79. C. Chatfield and G.R. Purdy: McMaster University, Hamilton, ON, Canada, unpublished research, 1976.
80. M. Guttmann and D. McLean: *Interfacial Segregation*, ASM, Metals Park, OH, 1979, p. 261.
81. M. Enomoto, C.L. White, and H.I. Aaronson: *Metall. Trans. A*, 1988, vol. 19A, p. 1807.
82. G.R. Purdy, D.H. Weichert, and J.S. Kirkaldy: *Trans. TMS-AIME*, 1964, vol. 230, p. 1025.
83. J.R. Bradley, J.M. Rigsbee, and H.I. Aaronson: *Metall. Trans. A*, 1977, vol. 8A, p. 323.
84. J.R. Bradley and H.I. Aaronson: *Metall. Trans. A*, 1977, vol. 8A, p. 317.
85. H.I. Aaronson, H.A. Domian, and G.M. Pound: *Trans. AIME*, 1966, vol. 236, p. 768.
86. H.I. Aaronson, G. Spanos, R.A. Masamura, R.G. Vardiman, D.W. Moon, E.S.K. Menon, and M.G. Hall: *Mater. Sci. Eng.*, 1995, vol. B32, p. 107.
87. G.R. Purdy, W.T. Reynolds, Jr., and H.I. Aaronson: *Proc. Int. Conf. on Solid-Solid Phase Transformations '99*, M. Koiwa, K. Otsuka, and T. Miyazaki, eds., Japan Institute of Metals, Sendai, Japan, 1999, p. 1461.
88. J.B. Gilmour, G.R. Purdy, and J.S. Kirkaldy: *Metall. Trans.*, 1972, vol. 3, p. 3213.
89. G.R. Purdy: *Metall. Trans. A*, 2004, vol. 35A, p. 1185.